Surface Induced Crystallization in Ultra-High Modulus Polyethylene Fiber Reinforced Polyethylene Composite

ARTICLE *in* MACROMOLECULES · JUNE 1991

Impact Factor: 5.8 · DOI: 10.1021/ma00012a017

2 AUTHORS:

Hatsuo Ishida
Case Western Reserve University
448 PUBLICATIONS **12,896** CITATIONS
SEE PROFILE

Philippe Bussi
Case Western Reserve University
8 PUBLICATIONS **184** CITATIONS
SEE PROFILE

Surface-Induced Crystallization in Ultrahigh-Modulus Polyethylene Fiber Reinforced Polyethylene Composites

Hatsuo Ishida* and Philippe Bussi

Department of Macromolecular Science, Case Western Reserve University, Cleveland, Ohio 44106-1712

Received June 11, 1990; Revised Manuscript Received December 11, 1990

ABSTRACT: Surface-induced crystallization of a high-density polyethylene matrix on a gel-spun, ultrahigh-modulus polyethylene fiber has been investigated both qualitatively and quantitatively. Under the microscope, the fiber exhibits a very good nucleation ability as seen from a uniform transcrystalline zone. As a first approach, heterogeneous nucleation is assumed. The free energy difference function $\Delta\sigma$, as it appears in the classical theory of heterogeneous nucleation, is then calculated. Because of the very high nucleation rate, which prevents the direct observation of individual spherulites at the interface, a new approach based on induction time is used to obtain an estimate of the free energy difference function $\Delta\sigma$, which is calculated to be $\Delta\sigma = 0.3$ erg/cm^2. This very low value may be explained considering the similar lattice parameters for this polymer/substrate system. Crystallization by melt epitaxy rather than transcrystallization may be observed. A new way to quantify the nucleating ability of a substrate toward a polymer melt in relation to the expected morphology is also proposed.

Introduction

Ultrahigh-modulus polyethylene (PE) fiber reinforced polyethylene composites are of particular interest from both a practical and scientific point of view. The addition of a fiber with very high specific mechanical properties to a rather inexpensive and common matrix is an attractive combination. Moreover, polyethylene has properties that make it desirable for certain biomedical applications: chemical resistance, low coefficient of friction, resistance to fatigue, and hydrophobicity. An excellent review article on PE fibers detailing the different manufacturing routes, the fiber properties, its limitations, and the leading researchers in the field has been published elsewhere.[1] This composite is unique considering that the matrix and the fiber are chemically identical and differ only by their physical state. PE fibers are characterized by very high molecular weight, generally 1–5 million, whereas the high-density PE matrix employed in this study has a molecular weight of the order of 34 000. The high degree of chain orientation due to the gel-spinning process gives the fiber a higher melting point (150 °C) than that of a regular high-density polyethylene matrix (130 °C). It is therefore possible to crystallize the molten polymer onto the fiber in a certain temperature window. Because of the chemical similarity and perfect lattice matching, favorable conditions are expected for surface-induced crystallization.

A major disadvantage of polyethylene fiber is the poor interfacial adhesion it exhibits toward different matrices it has been coupled with in the past. These matrices were mostly thermosets such as epoxy resins[2,3] and little has been done to investigate the use of thermoplastic matrices. It is well-known that the mechanical properties of polymer composites depend strongly on the quality of the interface. A usual way to enhance adhesion is to chemically bond the fiber to the matrix. Unfortunately, chemical bonding is not a realistic solution in the case of PE/PE composites because of the chemical inertness of both the fiber and the matrix.

However, transcrystalline growth of a high-density PE matrix on a commercially available PE fiber (Spectra 900) has been recently reported by He and Porter.[4] Figure 1 is an example of transcrystallization in PE/PE composite

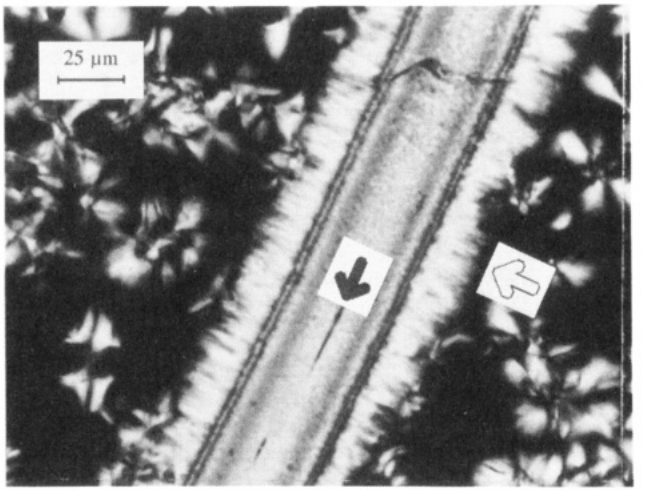

Figure 1. Transcrystalline growth (white arrow) of a linear high-density polyethylene matrix on an ultrahigh-modulus polyethylene fiber (black arrow). Isothermal crystallization (T = 126.5 °C, t = 15 min). The fiber is 38 μm in diameter.

and shows the growing transcrystalline zone (white arrow) on the PE fiber (black arrow). Individual spherulites can also be distinguished in the melt. The uniform transcrystalline growth front illustrates the high nucleating ability of the fiber toward the matrix. Because of the high density of nuclei on the fiber surface, the lateral development of the spherulites is impeded and growth can only proceed perpendicular to the fiber direction. Thus a columnar growth region is formed that extends to the spherulitic matrix.

This transcrystalline morphology is of particular interest because it has been advanced by several authors[5,6] that it leads to improved mechanical properties and adhesion. Campbell and Qayyum[7] have proposed that transcrystalline growth at the fiber surface is responsible for restrained necking of the fibers. Kwei et al.[8] and Matsuoka et al.[9] have shown that the modulus of the transcrystalline region is higher than that of the bulk phase. The results of Hsiao and Chen[10] indicate that transcrystallinity has a positive effect on the interfacial bond strength.

0024-9297/91/2224-3569$02.50/0

Numerous examples of transcrystallinity can be found in the literature whether the substrate is a film[11,12] or a fiber.[13,14] Most often optical microscopy has been employed, although transcrystallinity has been studied by differential scanning calorimetry,[4] X-ray diffraction,[15] and dynamic mechanical spectroscopy.[9] Because it is a nucleation-controlled process, transcrystallization depends strongly on thermodynamic conditions such as crystallization temperature or cooling rate. A review of the literature indicates that several other factors have an influence on the appearance of transcrystallinity: (1) Lattice matching and chemical similarity[4,14] between the fiber and the matrix play a role. Polymer chains can be preferentially adsorbed at the fiber surface, which facilitates the formation of stable heterogeneous nuclei. In this case the fiber can be viewed as a giant nucleating site. (2) The presence of a flow field due to processing conditions[16] is important. This creates a high degree of chain orientation near the fiber and promotes nucleation. (3) The surface free energy of the substrate[17] is a factor. The nucleation theory indicates that a high surface free energy substrate is more likely to induce heterogeneous crystallization. (4) The presence of a temperature gradient between the fiber and the matrix due to a mismatch in thermal conductivity[10] will have influence. A lower temperature at the fiber surface will increase the probability of nucleation. (5) Chemical composition of the fiber surface[14] may play a role. Strong interactions between the polar groups of the macromolecules and the fiber crystallites might be responsible for transcrystallization. (6) The presence of stresses at the interface fiber/matrix is another factor. These stresses can result from a difference in thermal expansion coefficient between the fiber and the matrix[18] or can be induced mechanically.[19] (7) It has also been proposed that the tendency toward transcrystallization depends upon molecular weight.[15]

However, despite extensive investigations most of the published work has been qualitative in nature and there is not always unanimity among authors concerning the influence of a particular parameter on transcrystallinity. In particular, few attempts have been made to quantitatively characterize the nucleating ability of a given substrate toward a given polymer melt. As shown later this is mostly due to a practical limitation of the theory of heterogeneous nucleation.

Therefore the goal of this paper is to investigate the energetics of the transcrystallization process using a modification of the theory of heterogeneous nucleation. This new approach, based on induction time, enables one to obtain an estimate of the free energy difference function $\Delta\sigma$ as it appears in the theory of heterogeneous nucleation. This approach is general and is not limited to the sole case of transcrystallization. The possibility of epitaxial nucleation (secondary nucleation) is also discussed. Last, a new way to quantify the nucleating ability for a given fiber/polymer melt pair based on the value of the free energy difference function is proposed.

Theory

(a) Theory of Heterogeneous Nucleation and Its Limitation When Applied to Surface-Induced Crystallization. The previous discussion has demonstrated the need for a more quantitative approach to surface-induced crystallization in PE fiber reinforced composites. Specifically one needs to know the amount of energy necessary to create a stable nucleus at the fiber surface and how this energy is affected by the various parameters mentioned earlier. At the length scale of a heterogeneous nucleus (a few hundred angstroms) the PE fiber can be treated as a flat surface. This model is very convenient because it has been used in most of the published studies[20,21] dealing with heterogeneous nucleation. Limitations of this model will be discussed later. Figure 2 presents the parameters defining the heterogeneous nucleus. a, b, and l represent the dimensions of the nucleus. σ is the side-surface free energy and σ_e is that for the fold surface (high-energy surface). The marked difference with the case of homogeneous nucleation is the introduction of $\Delta\sigma$, the interfacial free energy difference function. $\Delta\sigma$ is related to the creation of a new (al) top surface. A better understanding of the nature of $\Delta\sigma$ is achieved when it is related to its three basic components:[22]

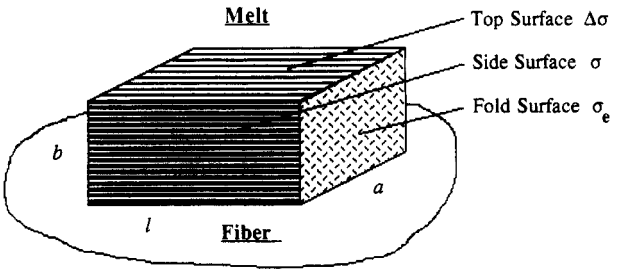

Figure 2. Parameters defining the heterogeneous nucleus.

$$\Delta\sigma = \gamma_{cs} + \gamma_{cm} - \gamma_{ms} \quad (1)$$

where γ_{cs} is the crystal–substrate interfacial free energy, γ_{cm} is the crystal–melt surface free energy ($\gamma_{cm} = \sigma$ as defined earlier), and γ_{ms} is the melt–substrate interfacial free energy. For hydrocarbons where dispersion forces are dominant (no polar interactions) Fowkes[23] further expressed γ_{ab} as $(\gamma_a^{1/2} - \gamma_b^{1/2})^2$, where γ_a and γ_b represent the dispersion components of the surface tension for phases a and b. In theory, $\Delta\sigma$ can be therefore brought down to the surface tension properties of the fiber, polymer crystal, and polymer melt. Because of this multiple dependency, $\Delta\sigma$ is a convenient way to define the nucleating ability of the PE fiber toward the PE melt. A lower value of $\Delta\sigma$ indicates a more favorable nucleation process. However, it is well-known that unless special precautions are taken,[24] heterogeneous nucleation of the PE melt will occur. The transcrystallization process has then to compete with bulk nucleation in the matrix. In the following $\Delta\sigma$ refers to the fiber/crystallite system whereas $\Delta\sigma'$ refers to the crystallite/heterogeneities in the melt system. Clearly, the relative magnitudes of $\Delta\sigma$ and $\Delta\sigma'$ influence the whole nucleation in the composite sample and its final morphology. In an effort to rationalize the classification of substrate activity first introduced by Chatterjee,[11] one can define the advantage A for a polymer to crystallize at the fiber surface rather than in the bulk as the ratio of $\Delta\sigma'$ and $\Delta\sigma$:

$$A = \Delta\sigma'/\Delta\sigma \quad (2)$$

The following three situations are encountered:

(1) $A \approx 0$ ($\Delta\sigma \gg \Delta\sigma'$): inactive substrate. The polymer melt ignores the presence of the fiber and there is no nucleation at the fiber surface.

(2) $0 < A < 1$: moderately active substrate. Spherulitic surface morphology is observed. Transcrystallinity becomes more probable as A approaches 1.

(3) $A \geq 1$: very active substrate. Nucleation is heavily favored at the fiber surface. Transcrystallinity is observed.

In order to calculate A, one needs to perform a combined growth and nucleation rate experiment. According to the

theory of polymer nucleation[25] the rate of heterogeneous nucleation is given by

$$I = I_0 \exp\left(-\frac{\Delta\varphi}{kT}\right) \exp\left(-\frac{\Delta G^*}{kT}\right) \tag{3}$$

where I_0 is a constant nucleation rate, $\Delta\varphi$ is the activation energy for a molecule to cross the phase boundary, and ΔG^* is the critical excess free energy due to the creation of a nucleus. k is Boltzmann's constant and T is the crystallization temperature. ΔG^* can be further expressed as

$$\Delta G^* = \frac{16\sigma\sigma_e\Delta\sigma T^{\circ}{}_m{}^2}{\Delta T^2 \Delta h_f{}^2} \tag{4}$$

where σ, σ_e, and $\Delta\sigma$ have been defined above. Δh_f is the heat of fusion per unit volume of crystal at the equilibrium melting point $T^{\circ}{}_m$, and ΔT is the supercooling degree. The nucleation rate can be then rewritten as

$$I = I_0 \exp\left(-\frac{\Delta\varphi}{kT}\right) \exp\left(-\frac{16\sigma\sigma_e\Delta\sigma T^{\circ}{}_m{}^2}{kT\Delta T^2 \Delta h_f{}^2}\right) \tag{5}$$

The growth rate is given by

$$g = g_0 \exp\left(-\frac{\Delta\varphi}{kT}\right) \exp\left(-\frac{\beta b_0 \sigma\sigma_e T^{\circ}{}_m}{kT\Delta T\Delta h}\right) \tag{6}$$

where g_0 is a constant growth rate and b_0 is the thickness of a new layer. b_0 can be related to the Miller indices of the polymer unit cell (for PE, $b_0 = d_{110}$). β is a constant characterizing the regime of growth: for regime I, $\beta = 4$ whereas for regime II, $\beta = 2$. In regime I, the completion of a new layer is rapid compared to the rate of nucleation whereas in regime II, multiple nucleation occurs at the substrate surface before a layer is completed. Since regime II requires a higher nucleation rate, it is observed at higher supercooling. It should be mentioned here that the activation energy $\Delta\varphi$ has a much smaller influence on the nucleation rate than the term due to the free energy difference $\Delta\sigma$, and particularly at low supercooling where the mobility of the polymer chains is still high. In the treatment of data, a WLF type of temperature dependency is often assumed.[26] By looking at eqs 5 and 6, one can readily see that the nucleation rate is a function of $1/(T\Delta T^2)$ whereas the growth rate depends on $1/(T\Delta T)$. A plot of $\ln I + \Delta\varphi/kT$ versus $1/(T\Delta T^2)$ should yield a straight line whose slope K_i is proportional to $\sigma\sigma_e\Delta\sigma$. Similarly, a plot of $\ln g + \Delta\varphi/kT$ versus $1/(T\Delta T)$ should yield a straight line whose slope K_g is proportional to $\sigma\sigma_e$. A combined nucleation and growth experiment thus yields estimates of $\sigma\sigma_e\Delta\sigma$ and $\sigma\sigma_e$ from which $\Delta\sigma$ is obtained.

However attractive, the approach described above has a very serious limitation when applied to the study of transcrystallization because the crowding of spherulites at the fiber surface makes any quantification of individual spherulites impossible. Therefore the nucleation density cannot be obtained. Consequently, the theory is restricted at this stage to polymer/substrate pairs with a certain window of $\Delta\sigma$, i.e., when A is much smaller than 1. Therefore if one wants to investigate truly transcrystalline growth, one has to find another route.

(b) The Induction Time Approach. The temperature dependency of the rate of heterogeneous nucleation I has been previously described by eq 5. I represents a number of nuclei per unit time per unit volume. In an isothermal experiment, a constant value is predicted. Thus the number of nuclei observed under the microscope in a given volume should be linear with time and nucleation should start at $t = 0$. However, this is not what it is typically observed. Generally an S-shaped curve is obtained with a certain delay before the onset of massive nucleation occurs (Figure 3). This delay is often called induction time t_i and is defined as the time intercept axis of the slope of the nucleation curve. Just as I varies with temperature so does t_i. However, these variations are in opposite directions. As the supercooling is decreased, the size of the critical nucleus becomes larger and the time required to create a stable nucleus increases. At the same time the nucleation rate decreases. Thus, intuitively one can feel that the induction time and the nucleation rate are related and carry the same information on the energetics of the system. This is of particular interest in the case of surface-induced crystallization because the time at which massive nucleation occurs can still be recorded even though individual spherulites cannot be distinguished at the fiber surface. Thus if one can relate t_i and I, $\Delta\sigma$ could be obtained even though I cannot be measured. Because I varies inversely with t_i, it seems natural to propose that the product of these two quantities is a constant. Mathematically:

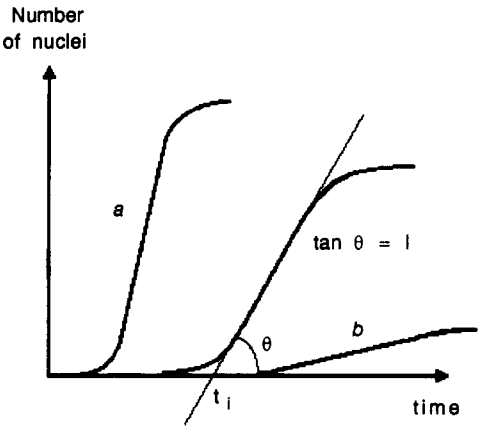

Figure 3. Definition of the nucleation rate I and of the induction time t_i. (a) Rapid nucleation, $I \to \infty$ and $t_i \to 0$. (b) Slow nucleation, $I \to 0$ and $t_i \to \infty$.

$$I(T)\, t_i(T) = K = \text{constant} \tag{7}$$

A theoretical justification of this relationship based on the Zeldovich–Becker–Döring theory of nucleation as well as the assumptions made to derive this relationship can be found elsewhere.[27] This approach is summarized in the Appendix.

Equation 7 has still a physical meaning in the following two extreme situations. For infinitely long nucleation (very low supercooling), the induction time goes to infinity as the nucleation rate is almost zero, but the product of these two quantities can still be a finite constant. Inversely, for almost immediate nucleation (very high supercooling), the nucleation rate goes to infinity as the induction time goes to zero (Figure 3). By looking at eq 7 and recalling eq 5, one can see that a plot of $\ln I + \Delta\varphi/kT$ or $\ln (1/t_i) + \Delta\varphi/kT$ versus $1/(T\Delta T^2)$ should yield a linear curve with the same slope K_i. It has been shown earlier that K_i is related to $\sigma\sigma_e\Delta\sigma$. Thus the temperature dependency of the induction time for transcrystallization to appear will yield $\Delta\sigma$. A classical nucleation rate study on the bulk matrix will yield $\Delta\sigma'$, and from this the ratio A as defined by eq 2 can be obtained.

Table I
Molecular Weight Distribution of the Fractions Used in This Study

fraction	M_w	M_n	polydispersity
F1	3300	1900	1.74
F2	4350	2350	1.86
F3	13000	4000	3.25
F4	31300	11100	2.82

Experimental Section

The linear high-density polyethylene (LHDPE) used as a matrix was a commercial product LS 630 formerly produced by USI Chemicals and now by Quantum Chemicals Co. This polymer has a weight-average molecular weight of 39 300 and a polydispersity of 3.38. The gel-spun, ultrahigh-modulus polyethylene fiber, Spectra 900, was supplied by Allied-Signal Co. The fiber was extracted for 20 h in a Soxhlet apparatus using chloroform as a solvent to remove the protective coating applied by the manufacturer and then dried in an oven at 70 °C for 20 h. Different fractions of LHDPE were obtained by the temperature-lowering method (Penning's fractionation[28]). A solution of the polymer in xylene was heated to 125 °C and then cooled to a temperature such as $82 < t$ °C < 93. The solution was sheared for 24 h. The stirrer was then removed and the precipitated material was allowed to deposit for another 24 h. The fractions were filtered two times to remove impurities and washed with ethanol and ethyl ether to remove the xylene. They were allowed to dry overnight at 100 °C. Each fraction was characterized by high-temperature (120 °C) gel permeation chromatography using o-dichlorobenzene as a solvent. The results are shown in Table I.

Composite films were prepared in a Mettler FP 82 hot stage by adding a fiber to a molten PE film deposited on a glass slide. Crystallization was observed with a Carl Zeiss optical microscope equipped with cross polarizers. A Nikon AFX II camera is attached to the optical microscope. The hot stage was calibrated with thermal standards. For the growth rate study, the film was cooled from 136 °C to the crystallization temperature at the rate of 10 °C/min. Once crystallization had occurred, the film was taken back to 136 °C and allowed to stand there for 15 min before being cooled again to a new crystallization temperature. Pictures of the transcrystalline growth front and sides were obtained from which measurements can be made. The use of slightly depolarized light allows one to clearly see the limit of the growth front. For the nucleation rate study in the bulk matrix, the number of nuclei per unit area was counted directly. The same constant area was kept under observation throughout the experiment. The PE film was initially kept at 180 °C for 1 h before being cooled to the crystallization temperature at the rate of 10 °C/min. Between each experiment the film was taken back to 180 °C for 15 min to minimize the effect of thermal history.

Results

(a) Qualitative Description. Figure 1 illustrates the high nucleating ability of the PE fiber toward the PE melt as can be seen from the uniform growth front of the transcrystalline zone. The thickness of the transcrystalline zone is of the order of 15 μm, the fiber being 38 μm in diameter. It is important to note that transcrystallization is a nucleation-controlled process. In particular, any change in the matrix morphology will be reflected in the texture of the transcrystalline zone. It has been reported in the literature[5,29] that a reduction in the matrix spherulite size decreases the extent of the transcrystalline zone. Additional evidence showing that the growth process is similar was produced by Chatterjee,[30] who measured the growth rates for the two processes and showed that they were indeed equal. It will be shown later that quantitative analysis of the transcrystalline growth rate leads to a numerical value for the parameter $\sigma\sigma_e$ in very good agreement with other studies done in the bulk.

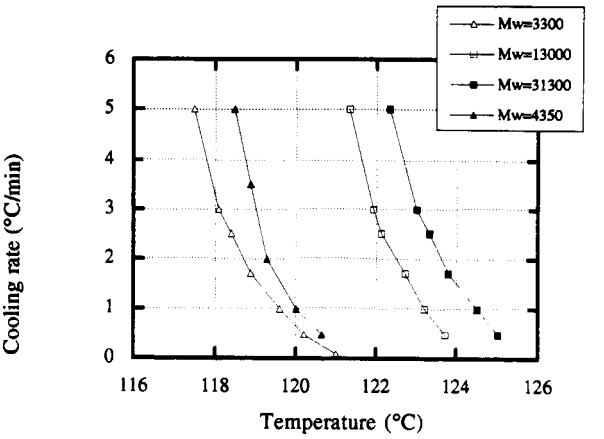

Figure 4. Influence of cooling rate and molecular weight on the transcrystallization temperature.

Once the fiber and the matrix have been chosen, molecular weight along with thermodynamic variables (supercooling and cooling rate) are the only parameters left to be modified. Molecular weight is of particular interest because it influences the crystallization temperature (i.e., the nucleation rate) as well as other properties, including wetting and viscosity. The wetting behavior influences the energetics at the interface whereas the viscosity influences the processing conditions. Additionally, the polydispersity of the sample is another factor because it leads to a distribution of crystallization temperatures. In this case the higher molecular weight fraction may serve as a nucleating agent for the lower molecular weight material. Last, molecular weight also influences the final morphology of the sample, because it controls in part the size of the spherulites.[31]

To investigate the influence of molecular weight and cooling rate on the crystallization behavior, composite films were prepared from fractionated samples. The films were cooled at various cooling rates, and the temperature at which transcrystallization appeared was recorded. The results are shown in Figure 4. Expectedly, a higher cooling rate creates a temperature lag because one is further away from an equilibrium situation. It is important to notice that a change in molecular weight of about 30 000 (from fraction F1 to fraction F4) induces a change in crystallization temperature of about 5 °C, the larger molecular weight crystallizing first. For the larger chains, less configurational entropy is lost during the phase transition. This corresponds to a lower value of the free energy for a critical nucleus (or to a smaller volume) and therefore to a higher crystallization temperature. It appears therefore that the width of the processing window depends on molecular weight. The temperature range available for crystallization is larger for the low molecular weight fraction but unfortunately the composite films produced in this case exhibit a brittle behavior. In the range of molecular weight and cooling rate investigated the fiber was found to always induce transcrystallinity. However, two particular morphologies were observed in the following cases.

For a molecular weight of 3300 the morphology in the matrix changes from mature spherulites to immature spherulites[31] (sheaflike spherulites). That is, growth occurs along diverging radial fibrils before filling the space uniformly (Figure 5). In this case the transcrystalline zone is expected to show a lesser degree of order and to contain more defects. In particular, the transcrystalline growth front appears to be less regular in this case than for the unfractionated polymer (Figure 1).

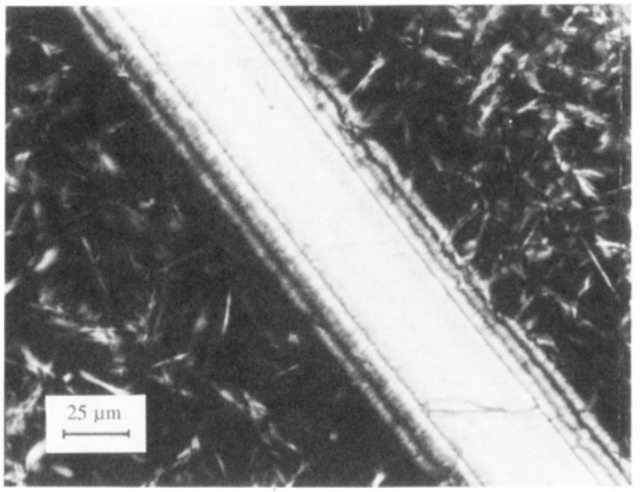

Figure 5. Immature or sheaflike spherulites observed for a low molecular weight fraction (M_w = 3300).

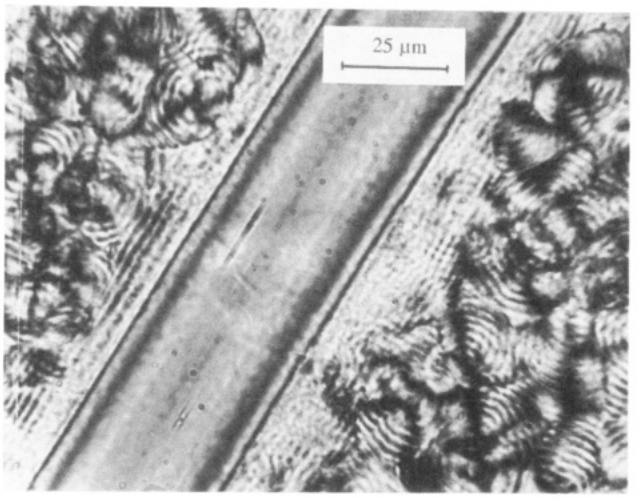

Figure 6. Banded transcrystalline zone observed as a result of rapid cooling of the composite film in air. Notice the parallel extinction lines near the fiber surface.

In another experiment a regular transcrystalline film was first produced by using the unfractionated polymer. The cover glass slide was then removed to avoid any optical effect and the composite film was remelted. The sample was then quenched in air and the resultant morphology was observed under the microscope. In this case banded spherulites were observed in the bulk matrix (Figure 6) as can be seen from the concentric extiction rings. This in turn results in a banded transcrystalline zone as seen from the presence of extinction lines parallel to the fiber direction. These lines arise from cooperative twists in the lamellae as a result of the induced thermal stresses.[31]

The important point in these two experiments is that a change in the matrix morphology is immediately reflected in the morphology of the transcrystalline zone. Therefore it seems essential to study the nucleation step because once nucleation has occurred, growth in the matrix and on the fiber proceeds in exactly the same way. In particular, the extent of the transcrystalline zone is not an indication on the nucleating ability of the fiber toward the melt.

(b) Growth Rate Study on the Transcrystalline Zone. By performing the growth rate study on the transcrystalline zone rather than on the bulk spherulites, one can verify that the equations developed for this latter case are still valid when applied to transcrystallization. At the present time, there are little data in the literature on the transcrystalline growth rate. PE is a convenient choice because extensive data on the spherulitic growth rate are available for comparison. Moreover, the measurements are made more easily and more precisely since a uniform growth front is observed. For a given crystallization temperature, pictures were taken at different times and developed into slides from which the extent of the transcrystalline zone is measured. The data were collected in two successive experiments. Each rate (in μm/s) is obtained from no less than four points. The thickness of the transcystalline zone was found to increase linearly with time. The chosen crystallization temperatures ranged from 124.1 to 128.4 °C. In this range the growth rate changes by a factor of approximatively 700 ($g_{124.1} \approx 0.0664$ μm/s and $g_{128.4} \approx 0.0001$ μm/s). At the same time the transport term $\Delta\varphi/kT$ is practically constant and can be neglected in the treatment of the data. The plot of ln g versus $1/(T\Delta T)$ is shown in Figure 7 and exhibits a regime II behavior for the first 10 temperatures. The following values taken from the literature[32] were used in the treatment of the data: $\Delta h_f = 2.8 \times 10^9$ erg/cm^3, $T^\circ_m = 416$ K, and $b_0 = 4.1$ Å. The quoted value for T°_m was selected to compare the present data with the data obtained by Hoffman, Davis, and Lauritzen.[26] The actual equilibrium melting point is probably closer from 418.2.[33,34] From the value of the slope, $\sigma\sigma_e$ was calculated to be 1380 erg^2/cm^4, in good agreement with other independent estimates for bulk spherulites where the average value of 1310 erg^2/cm^4 has been reported.[26] Thus it appears that transcrystalline growth rate data can be used safely for the determination of the free energy parameters. The values of g at higher temperatures are believed to follow a regime I behavior where 127.3 °C would be the breaking point. Indeed the calculated slope using these points was found to be 26.0×10^4 K^2, roughly twice the value for regime II (12.2×10^4 K^2) as expected from the theory. This would be in good agreement with the work of Hoffman, Davis, and Lauritzen on a fraction of similar molecular weight.[26] At higher temperatures, the presence of axialites in the polymer melt along with regular spherulites was observed. Axialites, which appear as immature spherulites with thicker and more diffuse branches, are characteristic of a regime I behavior. However, there is no change in the morphology of the transcrystalline zone. Nonetheless the absolute value of the transcrystalline growth rate is sensitive to this change in morphology. It is believed that the value of the slope found for regime I is artificially high because molecular weight segregation may occur in the melt with adsorption of the low molecular weight fraction onto the fiber. As mentioned earlier, the presence of low molecular weight material near the fiber surface will delay the appearance of transcrystallization and slow down the

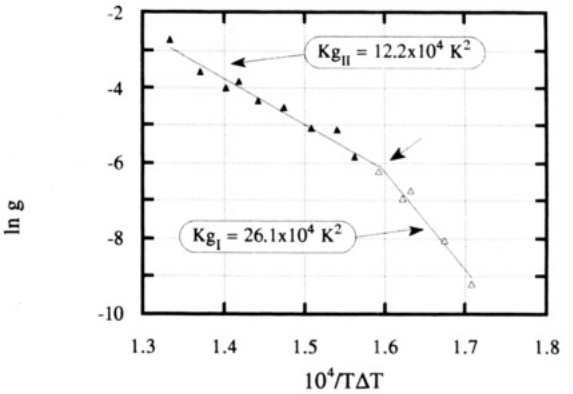

Figure 7. Plot of ln g versus $1/(T\Delta T)$. The change in growth regime is indicated by the arrow.

Table II
Transcrystalline Induction Time Data

T, °C	124.65[a]	125.1	125.6	126.0	126.4	126.5	127.0	127.3	127.6
t_i, s	40	60	100	150	200	270	420	780	1080

[a] Average value over the duration of the experiment.

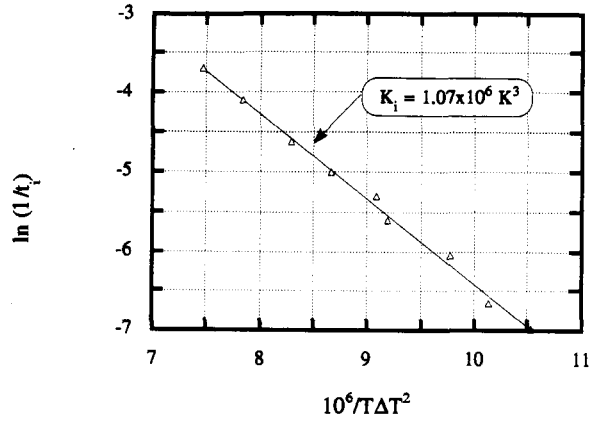

Figure 8. Plot of ln $(1/t_i)$ versus $1/(T\Delta T^2)$.

growth process.

During the first growth rate experiment, the induction time for the transcrystalline zone to appear was also recorded visually with a chronometer. It was first attempted to obtain the induction time value from the zero-thickness extrapolation of the plot of the transcrystalline growth thickness versus time. However, an exact measurement of the fiber diameter is hard to obtain because it is very difficult to focus exactly on the fiber contour. This is due to the fact that the diameter of the crystalline PE fiber is quite important (38 μm) and that it acts as a prism by diffracting light. As a result the fiber contour appears to be dark by contrast to the bright central part of the fiber. However, upon transcrystallization, a distinct fine line of light will appear next to the dark area, and the induction time can then be recorded. For a noncrystalline fiber or a fiber with a smaller diameter, the zero-thickness intercept method is certainly preferable.

The results are presented in Table II. Large differences can be observed for a change in temperature of a few degrees. When these data are plotted as ln $(1/t_i)$ versus $1/(T\Delta T^2)$ a straight line is obtained (Figure 8). Before using these results to estimate the value of $\sigma\sigma_e\Delta\sigma$, one has to test the induction time hypothesis (eq 7) on a system where $\Delta\sigma$ can be measured from both the nucleation rates and the induction times. It was decided to carry out the experiment on the bulk PE matrix because this will also provide an estimate of the free energy difference function in the melt $\Delta\sigma'$. This allows one to compare the respective nucleating ability of the fiber and the heterogeneities present in the melt which are responsible for the bulk nucleation.

(c) Nucleation Rate Experiment and Verification of the Induction Time Hypothesis. For this experiment the number of nuclei was counted by direct observation on the bulk PE matrix. The same constant area was kept under observation at temperatures ranging from 126.2 to 127.8 °C. In this range the nucleation rate (in number of nuclei per unit area per s) and the induction time change by a factor of approximately 20. The nucleation curves generally display an S shape (Figure 9). The induction times were obtained by the time-axis intercept of the slope of each nucleation curve. Figure 10a is a plot of ln I versus $1/(T\Delta T^2)$ and gives a value of 1.28×10^6 K^3 for K_i. From this a true value of 0.4 erg/cm^3 is obtained for $\Delta\sigma'$ using the $\sigma\sigma_e$ estimate from the growth rate study. However,

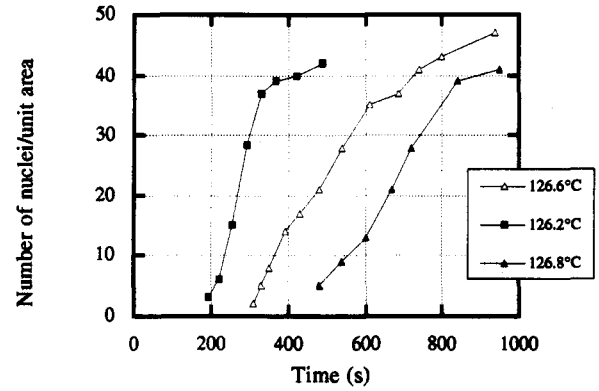

Figure 9. Typical bulk matrix nucleation curves.

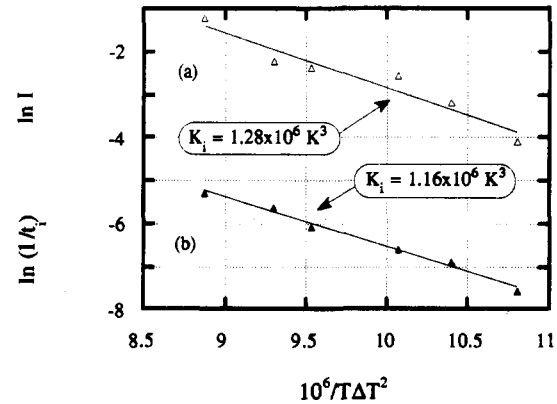

Figure 10. Test of eq 7 by comparison of (a) the nucleation rate approach and (b) the induction time approach.

Table III
Comparison of the Nucleating Ability for Different Polymer/Substrate Pairs (Heterogeneous Nucleation Analysis)

polymer/substrate	$A = \Delta\sigma'/\Delta\sigma$	morphology
poly(1-butene) polystyrene (film)[a]	0.5	spherulitic
poly(1-butene) polypropylene (film)[a]	0.6	spherulitic
polyethylene polyethylene (fiber)	1.3	transcrystalline
poly(ϵ-caprolactone) polyethylene (fiber)[b]	2.0	transcrystalline

[a] Reference 20. [b] Reference 27.

the important point here is that a similar plot for the induction times yields a value of the slope in fair agreement (1.16×10^6 K^3 versus 1.28×10^6 K^3, i.e., a 9% difference) with the value obtained from the nucleation rate and with an excellent linear correlation (Figure 10b). Thus the assumption made earlier appears to be justified, and one can now use the results of Figure 8 to deduce $\Delta\sigma$. Part of the difference between the value of K_i determined from two approaches is due to the uncertainty on the origin of time. A way to estimate this correction has been proposed elsewhere.[27] From the value of K_i, $\Delta\sigma$ was estimated to be of the order of 0.3 erg/cm^3. The results are summarized in Table III along with value obtained from the literature[20] and from another study.[27]

Discussion

In this study the value of the free energy difference function for the fiber ($\Delta\sigma$ = 0.3 erg/cm^2) and the melt ($\Delta\sigma'$

= 0.4 erg/cm^2) was determined. To our knowledge no other independent estimate is available for this PE/PE system. These two parameters are a measure of the nucleating ability of the fiber and of the heterogeneities in the melt. The ratio of these two quantities gives an indication of the expected morphology of the composite film. The question is: how does the PE/PE system compare to other systems and what does it mean for the nucleation process?

A review of the literature indicates that few data of this type are available. This can be explained considering the following: in the nucleation density approach one has to be able to count the number of individual spherulites in order to obtain $\Delta\sigma$ for a given polymer/substrate system. This can only be done when the nucleation density is moderate, i.e., when in fact no uniform transcrystalline zone can be seen but rather a few spherulites impinging on each other. Thus this type of approach is restricted to systems with a certain window of $\Delta\sigma$. In a study of 43 substrate/polymer pairs Chatterjee[20] selected adequate systems and found the following values: $\Delta\sigma$ = 2.18 erg/cm^2 for poly(1-butene) crystallizing on isotactic polystyrene, $\Delta\sigma$ = 2.04 erg/cm^2 for the same polymer in contact with isotactic polypropylene, and $\Delta\sigma'$ = 1.16 erg/cm^2 for the bulk heterogeneities in the poly(1-butene). These values are considerably higher than the values obtained for PE/PE composites. Therefore, it can be concluded that the nucleating ability of ultrahigh-modulus polyethylene fiber toward a linear high-density polyethylene matrix is very high. The low value obtained for $\Delta\sigma'$ also indicates that there is a stiff competition from the matrix. The small difference between $\Delta\sigma$ and $\Delta\sigma'$ should not be underestimated: this difference in energy is equivalent to a change of about 1 °C for the nucleation rate (this estimate is obtained by setting: $\Delta\sigma/(T\Delta T^2) = \Delta\sigma'/(T'\Delta T'^2)$ and ΔT = 17 °C; this gives $\Delta T' \approx 18$ °C).

To understand why $\Delta\sigma$ is so low, one can use eq 1 and the Fowkes expression for the interfacial free energy. Extended-chain fibers such as PE fiber exhibit a very high degree of orientation (95–99%) and crystallinity (60–85%). Analysis of an X-ray fiber diffraction pattern obtained in our laboratory confirmed that the fiber has the same lattice parameters as the polyethylene matrix. Thus epitaxial crystallization (the *c* axis of the polyethylene matrix is along the fiber axis and the *b* axis is orthogonal to the fiber direction) is a distinct possibility that would be energetically favorable. Because of the perfect lattice matching and the chemical similarity, one can reasonably expect γ_c and γ_s to be nearly equal. In this case $\gamma_{cs} \approx 0$, $\gamma_{cm} \approx \gamma_{ms}$, and consequently $\Delta\sigma$ can be very low. Therefore little energy is needed to create a new (*al*) surface. It is interesting to note that a zero value for $\Delta\sigma$ would mean that secondary nucleation occurs, which of course is the limiting case. One should note, however, that the chemical similarity between the substrate and the fiber does not imply necessarily that $\gamma_c = \gamma_s$. Indeed Schonhorn and Ryan[35] have shown that the surface tension of PE single crystals (on the order of 66 erg/cm^2) is very different from that of an amorphous surface layer (on the order of 36 erg/cm^2). Therefore the free energy of formation of a nuclei on a PE crystal or on a PE fiber is not necessarily the same. If nucleation followed by transcrystallization occurs, then the *c* axis is not necessarily along the fiber direction. In this case the lattice matching is perturbed and $\Delta\sigma$ is expected to be larger than for epitaxial crystallization.

In any case the low value found for $\Delta\sigma$ indicates the likelihood of epitaxial crystallization in PE/PE composites. Due to the high degree of crystalline orientation the fiber can be furthermore regarded as a giant nucleating site. These two factors combined to ensure a transcrystalline morphology under various thermodynamic conditions. However, due to imperfections on the fiber surface, the possibility of nucleation immediately leading to transcrystallization cannot be ruled out. Epitaxial crystallization produces lamellae growing perpendicular to the fiber direction. The fiber roughness can be expected to cause these lamellae to impinge as one is further away from the fiber surface, thus disrupting their order and randomizing the orientation of the *c* axis. Thus one may have both processes occurring simultaneously.

At this point one should also make a general remark concerning the assumption of a finite number of nucleation sites. This assumption is probably violated as the free energy difference function approaches zero. In this case indeed, the whole substrate can become a nucleation site and the notion of an upper bound to the total number of nuclei disappears. In particular, this approach is not appropriate to test secondary nucleation ($\Delta\sigma$ = 0), as eq 9 in the Appendix is no longer valid.

Last, a few comments should be made about the theory of heterogeneous nucleation. In principle, once σ, σ_e, and $\Delta\sigma$ are known, it is possible to determine the dimensions of the critical nucleus. The value found for $\Delta\sigma$ indicates that the thickness of the nucleus is less than that of a monomolecular layer, which is clearly impossible. This means in fact that the critical free enthalpy found for the creation of nuclei is less than predicted by the theory. A possible explanation for this is that the critical nuclei at the fiber surface do not have their predicted equilibrium shape. Indeed, because of the energetically favored process, many nuclei can be nucleated simultaneously. They may therefore impinge on each other before reaching their predicted dimensions. This would explain in particular why transcrystalline lamellae have been found to melt before bulk lamellae.[9] It should also be kept in mind that the equations used to predict the shape of the critical nucleus have been derived assuming that each dimension can be treated as a continuous function of the number of crystallizing elements. Clearly, this is not the case when the nucleation is so favored that an adsorbed chain folding onto itself can be stable enough to be a nucleus. Thus the model used in this study is useful for comparison of the nucleating ability of different polymer/substrate pairs but one should not emphasize the prediction concerning the equilibrium dimensions of a nucleus.

Conclusions

(1) Polyethylene fibers were found to exhibit a very good nucleating ability toward LHDPE as seen from a uniform transcrystalline growth front.

(2) Growth rate study on the transcrystalline zone provided an estimate of $\sigma\sigma_e$ in very good agreement with data obtained on bulk spherulites.

(3) Using an approach based on induction time, it was possible to determine the free energy difference function, $\Delta\sigma$, for the fiber/melt system. This parameter is not otherwise accessible by the nucleation rate method because the individual nuclei in the transcrystalline zone cannot be distinguished.

(4) $\Delta\sigma$ was found to be on the order of 0.3 erg/cm^2. This very low value indicates that transcrystallization is energetically favored.

(5) It is believed that nucleation may occur by melt epitaxy because of the highly favorable energetics of this process. However, both epitaxial crystallization and trans-

crystallization may be present. Further work is needed to investigate the degree of order in the transcrystalline zone perpendicular to the fiber direction.

(6) The model developed in the theory of heterogeneous nucleation is useful only for comparison. It does not predict a realistic geometry for the critical nucleus.

Acknowledgment. This work was in part supported by the Office of Naval Research. We are grateful to Dr. C. D. Lee of Quantum Chemicals Co. for the high-temperature GPC measurements.

Appendix

To derive eq 7 one has to understand first why an induction time is observed. The nucleation rate in eq 5 is a steady-state nucleation rate. It is assumed that, at the crystallization temperature considered, there is an equilibrium size distribution of subcritical nuclei (embryo). Following the notations used by Frisch,[36] $f(g,t)$ represents the distribution function of embryo of size g at time t. As suggested by Wunderlich,[25] this distribution can be represented by a decreasing exponential: it is much more probable to find numerous small embryos in the melt than a large embryo because the free enthalpy necessary for a large embryo to survive is greater. In an isothermal nucleation experiment the sample is generally quickly cooled from T_i (initial melt temperature, far above the equilibrium melting point) to T_c (temperature of crystallization). The induction time, t_i, is the time necessary to reach the steady-state distribution at T_c, $f_{s,T_c}(g)$ starting from an initial steady-state distribution at T_i, $f_{s,T_i}(g,0)$. Using the ZBD theory of nucleation (Zeldovich;[37] Becker and Döring[38]), Frisch showed that

$$t_i(T) = [1/I(T)] \int_0^G [f_{s,T_c}(g) - f_{s,T_i}(g,0)]\, dg \qquad (8)$$

where G is the size of the embryo for which the probability of decomposition is essentially zero (G is slightly larger that g^*, the size of a critical nucleus). At this point one should mention that the ZBD theory was initially derived for what is termed self-nucleation, i.e., nucleation that arises in the melt from its own previously grown crystals. Partially molten high molecular weight crystals can serve as seeds for self-nucleation. However, this theory can be applied to this study if the following remarks are made. In the case of heterogeneous nucleation, it is assumed that the subcritical nucleus initiates at the surface of the substrate or at the heterogeneities present in the melt. This is justified because it is easier for an embryo to survive on a foreign surface than in its own melt. In the case of transcrystallization the assumption of subcritical nuclei preferentially growing at the fiber surface rather than in the melt is even more justified because of the particular affinity between the matrix and the fiber. Therefore, if the concentration of heterogeneities is assumed to be constant for the temperature range $[T_1,T_2]$ investigated, one can write

$$\int_0^G f_{s,T_c}(g)\, dg = \text{constant}, \quad T_c \in [T_1,T_2] \qquad (9)$$

Equation 9 expresses that the number of particular embryos of size g can change from one temperature to the other but the total number of stable nuclei that are generated is a constant because there is only a fixed number of heterogeneities in the melt that can initiate nucleation. This is equivalent to a condition of normalization for a probability.

The second assumption made is that at the initial temperature T_i

$$f_{s,T_i}(g,0) = 0, \quad g \in [0,G] \qquad (10)$$

When T_i is far above T°_m and the melt is kept at this temperature a sufficient time, this assumption is reasonable. This means that at temperature T_i no embryo can survive at the interface melt/heterogeneities. With these two assumptions eq 7 can be derived as follows:

$$t_i(T) = \frac{\int_0^G [f_{s,T_c}(g) - f_{s,T_i}(g,0)]\, dg}{I(T)} = \frac{\int_0^G f_{s,T_c}(g)\, dg}{I(T)} = \frac{\text{constant}}{I(T)} \Rightarrow I(T)\, t_i(T) = K \qquad (11)$$

The following remark should be made: it has been assumed in eq 9 that the subcritical nuclei initiate at the surface of heterogeneities. However, one cannot totally dismiss the possibility of limited self-nucleation, i.e., subcritical nuclei surviving in the melt without the help of a foreign surface. Because the number of these nuclei is a decreasing function of temperature, a temperature dependency of K in eq 7 is possible. Experimentally, one can minimize this effect by preheating the melt far above the equilibrium melting point and by renewing this procedure in between each crystallization experiment. Another possible source of temperature dependency for K arises from the double assumption that $\Delta\sigma$ is the same for all the impurities present in the melt and that it does not vary with temperature. It is more likely that there is a distribution of $\Delta\sigma$ with nuclei becoming active or inactive as the crystallization temperature changes. Therefore the value of $\Delta\sigma$ calculated from the induction time experiment should be regarded as an average value. However, this is consistent with the expression for the nucleation rate (eq 5), which also assumes a constant value of $\Delta\sigma$.

References and Notes

(1) Weedon, G. C.; Tam, T. Y. *Mod. Plast.* **1986**, *63*, 64.
(2) Ladizesky, N. H.; Ward, I. M. *J. Mater. Sci.* **1983**, *18*, 533.
(3) Nardin, M.; Ward, I. M. *Mater. Sci. Technol.* **1987**, *3*, 814.
(4) He, T.; Porter, R. S. *J. Appl. Polym. Sci.* **1988**, *35*, 1945.
(5) Cheng, F. S.; Kardos, J. L.; Tolbert, T. L. *SPE J.* **1970**, *26*, 62.
(6) Kantz, M. R.; Corneliussen, R. D. *J. Polym. Sci., Polym. Lett. Ed.* **1973**, *11*, 279.
(7) Campbell, D.; Qayyum, M. M. *J. Mater. Sci.* **1977**, *12*, 2427.
(8) Kwei, T. K.; Schonhorn, H.; Frisch, H. L. *J. Appl. Phys.* **1967**, *38*, 2512.
(9) Matsuoka, S.; Daane, J. H.; Bair, H. E.; Kwei, T. K. *J. Polym. Sci., Polym. Lett. Ed.* **1968**, *6*, 87.
(10) Hsiao, B. S.; Chen, E. J. *Controlled Interphases in Composite Materials*; Ishida, H., Ed.; Elsevier Science: New York, 1990; p 613.
(11) Chatterjee, A. M.; Price, F. P.; Newman, S. *J. Polym. Sci.* **1975**, *13*, 2369.
(12) Weinhold, S.; Litt, M. H.; Lando, J. B. *J. Appl. Phys.* **1980**, *51*, 5145.
(13) Gray, D. G. *J. Polym. Sci., Polym. Lett. Ed.* **1974**, *12*, 509.
(14) Hobbs, S. H. *Nature Phys. Sci.* **1971**, *234*, 12.
(15) Lovering, E. G. *J. Polym. Sci., Part A-2* **1970**, *8*, 1697.
(16) Burton, R. H.; Day, T. M.; Folkes, M. J. *Polym. Commun.* **1984**, *25*, 361.
(17) Goldfarb, L. *Makromol. Chem.* **1980**, *181*, 1757.
(18) Thomason, J. L.; van Rooyen, A. A. *Controlled Interphases in Composite Materials*; Ishida, H., Ed.; Elsevier Science: New York, 1990; p 423.
(19) Gray, D. G. *J. Polym. Sci., Polym. Lett. Ed.* **1974**, *12*, 645.
(20) Chatterjee, A. M.; Price, F. P.; Newman, S. *J. Polym. Sci.* **1975**, *13*, 2391.
(21) Koutsky, J. A.; Walton, A. G.; Baer, E. *J. Polym. Sci., Polym. Lett. Ed.* **1967**, *5*, 185.

(22) Cherry, B. W. *Polymer Surfaces*; Cambridge University Press: London, 1981.
(23) Fowkes, F. M. *Ind. Eng. Chem.* **1964**, *56*, 40.
(24) Gornick, F.; Ross, G. S.; Frolen, L. J. *J. Polym. Sci., Part C* **1967**, *18*, 79.
(25) Wunderlich, B. *Macromolecular Physics*; Academic Press: New York, 1976; Vol. 2, Chapter 5.
(26) Hoffman, J. D.; Davis, G. T.; Lauritzen, J. I. *Treatise on Solid State Chemistry*; Hannay, N. B., Ed.; Plenum: New York, 1976; Vol. 3, Chapter 7.
(27) Ishida, H.; Bussi, P. *J. Mater. Sci.*, accepted.
(28) Pennings, A. J. *Recl. Trav. Chim. Pays-Bas* **1964**, *83*, 552.
(29) Fitchmun, D.; Newman, S. *J. Polym. Sci., Polym. Lett. Ed.* **1969**, *7*, 301.
(30) Chatterjee, A. M.; Price, F. P.; Newman, S. *J. Polym. Sci.* **1975**, *13*, 2385.
(31) Bassett, D. C. *Principles of Polymer Morphology*; Cambridge University Press: London, 1981.
(32) Gornick, F.; Hoffman, J. D. *Ind. Eng. Chem.* **1966**, *58*, 41.
(33) Hoffman, J. D. *Polymer* **1983**, *24*, 3.
(34) Hoffman, J. D. *Polymer* **1982**, *23*, 656.
(35) Schonhorn, H.; Ryan, F. W. *J. Phys. Chem.* **1966**, *70* (12), 3811.
(36) Frisch, H. L. *J. Phys. Chem.* **1957**, *27* (1), 90.
(37) Zeldovich, J. *J. Exptl. Theor. Phys.* **1942**, *12*, 525.
(38) Becker, R.; Döring, W. *Ann. Phys.* **1935**, *24* (5), 719.

Registry No. LS 630, 9002-88-4.